Key Engineering Materials *Online: 2011-10-27*
ISSN: 1662-9795, Vols. 493-494, pp 768-774
doi:10.4028/www.scientific.net/KEM.493-494.768

FTIR Analysis and Cytotoxicity Test of Titanium Dioxide Nanoparticles

Rodrigues, L.R.[1,2,3,4, a]; Dias, C.G.B.T.[1,2,5, b]; Ceragioli, H.J.[6, c]; Rodas, A.C.D.[7,d]; Monteiro, F.J.M.[3,4, e] and Zavaglia, C.A.C.[1,2, f].

[1]Department of Materials Engineering, Faculty of Mechanical Engineering, State University of Campinas, Campinas, São Paulo, Brazil;

[2]National Institute of Science and Technology in Biofabrication, Campinas, São Paulo, Brazil;

[3]Universidade do Porto, Faculdade de Engenharia, Departmento de Engenharia Metalúrgica e Materiais, Porto, Portugal;

[4]INEB-Instituto de Engenharia Biomédica, Porto, Portugal;

[5]Polymers Group, Institute of Technology, Faculty of Mechanical Engineering, Federal University of Para, Belem, Para, Brazil;

[6]Department of Semiconductors, Instruments and Photonics, School of Electrical and Computer Engineering, State University of Campinas, Campinas, São Paulo, Brazil;

[7]Institute of Nuclear Energy Research / National Nuclear Energy Commission – Center of Biotechnology, São Paulo, SP, Brazil.

[a]leo5002@fem.unicamp.br, [b]carmendias@fem.unicamp.br, [c]helder@desif.fee.unicamp.br, [d]arodas@ipen.br, [e]ffmont@ineb.up.pt, [f]zavagl@fem.unicamp.br

Keywords: Nanotechnology, sol-gel with sucrose, *Scherrer* equation, FTIR, Cytotoxicity test.

Abstract. Titanium dioxide is a material widely used in electronics industry and little explored in the biomedical area, which is the objective of this work. Nowadays one can find surgical instruments coated with thin films that have bactericidal properties when they are activated in the presence of ultraviolet light. For crystalline phase control TiO_2 was calcinated at 500°C. The crystallite mean size for sample calcinated at 500°C was 27nm. With the results of cytotoxicity it is possible to say that biomedical applications are possible. Electron microscopy images showed nanoparticles obtained by sol-gel process and the compounds were identified by FTIR analysis. Raman spectroscopy confirmed the existence of anatase titania phase and X-ray diffraction showed this material to be composed of a crystalline phase. X-ray fluorescence identified chemical contaminants.

Introduction

TiO_2 (titania) is a synthetic bioinert bioceramic used in biomedical applications, but this material can be used in another areas. It is well known that titanium oxide ceramics have good biocompatibility and hemocompatibility [1].

Al_2O_3, ZrO_2 and TiO_2 are bioinert materials designed to be used as dental, joint or bone implants. TiO_2 scaffolds are potential materials for implants, showing biocompatibility and capability to enhance bone ingrowth [2].

Titanium dioxide is used in food color additive and in correct dosages it has been used as cosmetic sunblock [3]. The most used pigment effect consists of mica flakes with TiO_2 and it can be used in automotive top coatings, plastics, printing inks, industrial coatings, and cosmetics, because of its eye-catching effects [4]. Rutile TiO_2 showed excellent results in removing heavy metals ions from aqueous solution due to its high adsorption affinity for metal ions [5]. TiO_2 can be used incorporated in biopolymer-based films for protection against foodborn micro-organisms and allergens in the presence of ultraviolet radiation [3]. Some studies indicate that nanoestrutured TiO_2 film can increase the corrosion resistance of titanium alloys, but further research is still required in this area [6].

Thin films of titanium oxides are used in solar-energy conversion based on photocatalytic, photovoltaic devices. For this application it is important to know that the thermodynamic phase stability of nanocrystalline aggregates during growth depends on initial particle size, but for equally sized particles, the anatase nanoparticles are thermodynamically stable for sizes below 11 nm, brookite is stable for sizes between 11 and 35nm and rutile is stable in sizes greater than 35 nm [7].

Nowadays tissue engineering applications are very attractive and many materials are being used for that purpose, including titania. Tissue engineering associated to nanotechnology are developing biological substitutes that restore, maintain or improve the original functions as bone regeneration [2]. The scaffolds used as structural support and substrate for cell adhesion are currently an important area of study [8] [9] and titania is an interesting biomaterial to include in these structures. The chemical composition, physical structure and biologically functional moieties are all import attributes to biomaterials for tissue. Several materials have been used as scaffolds, for example metals, polymers and ceramics. For tissue engineering a biomimetic scaffold should be a three-dimensioal structure, with interconnected porosity and with pore size between 100 and 400 microns. These structures facilitate cell seeding, adhesion, proliferation, differentiation and neo tissue genesis. The TiO_2 nanotube layer obtained by titanium anodizing has shown good results in biomaterial application and increased osteoblast cell adhesion in vitro and in vivo [6].

Titania is a good bonding coat, because it shows high corrosion resistance and it is an inert biomaterial, therefore, TiO_2 improves the interfacial bonding strength of the substrate and coating [10].

Nanotechology is an innovative concept with numerous technological advances, therefore it became the object of study by many researchers worldwide.

Nanotechnology associated with biotechnology is one of the most important emerging fields of science in this century [11]. The nanomaterials are all likely to have an impact on their potential toxicity depends on nanoparticle size and surface properties [12]. Nowadays, the countries are concerned with the possible environmental problems that could be caused by nanomaterials, but this work has shown bioinert nanoparticles. The nanostructures are based on bioinspired design performing necessary function at the right time and at the right place by manipulating molecules and atoms assembly to generate natural tissues, for example bone tissue.

In this work, the method used to produce pure TiO_2 was sol-gel with sucrose, but other processes are used too, as conventional sol-gel process, precipitation process, gas phase synthesis route [13], among others.

The incresed surface area of nanoparticle often leads to distinct values of reactivity, mechanical, chemical and biological properties *in vitro* and *in vivo* when compared to micro and macroscopic particles. The *in vivo* bone bioactivity of the TiO_2 was predicted in simulated body fluid (SBF) and transformed amorphous calcium carbonate into crystalline hydroxyapatite. This process was proposed as a new bio-inspired pathway toward bioactivity [2].

The objective of this study was to explore the characteristics of TiO_2 and the response to *in vitro* test.

Materials and Methods

$TiCl_4$ IV (≥99%, Merck, Germany) was used as the precursor of the TiO_2 powder. $TiCl_4$ was diluted in ethanol (99.5%, Synth, Brazil) in order to avoid its violent reaction when in contact with water. The volume ratio of ethanol/$TiCl_4$ used was, approximately, 4:1. Sucrose (Merck, Brazil) was used as a gel-forming agent.

Initially, an ethanol/sucrose solution was prepared (77.56% in volume of ethanol and 3.05% in volume of sucrose). Then, $TiCl_4$ was slowly added under vigorous stirring. After a while, the solution was heated to 80°C until a black gel-like slurry was formed. Afterwards, the slurry was dried at 100°C to form a fine black powder. Finally, the sample was calcinated at 500°C for 1 hour.

Powder Characterization. Samples' crystalline phases and crystallite size were determined by X-ray powder diffraction (XRD) using a Rigaku DMAX 2200 diffractometer provided with Cu-Kα radiation and Ni filter. The 2θ range analyzed was 20° - 90°, with a step-size of 0,02° and a counting time of 1 s per step. JCPDS data used to identify the crystalline phases were 21-1272 and 04-0477 for anatase titania.

Crystallite size was calculated using *Scherrer* Equation [14] (Eq.1) after fitting a Gaussian curve on the main peaks of the diffraction pattern to determine their width at half height intensity [15].

$$t = 0{,}9\lambda / \beta\cos\theta. \quad (1)$$

Where, t is crystallite mean size, λ is X-ray wavelength, β (given by Eq. 1) is peak width at half height intensity, and θ is Bragg angle.

$$\beta = \beta^2_{exp} - \beta^2_{inst.} \quad (2)$$

Where, β_{exp} is the sample's peak width at half height intensity and β_{inst} is the instrumental correction obtained by the width at half height intensity of the monocrystal pattern (Eq. 2).

Fourier Transformed Infrared Analysis. Infrared spectra analysis was performed with a Fourier Transform Infrared Spectroscopy (FTIR) and the equipment used was a Thermo Scientific Nicolet IR100 FT-IR spectrometer with spectral resolution between 128 to 4 cm^{-1}. The spectral range used was 800 to 400 cm^{-1}. For these analyses the samples were deposited in surface of windows for spectrophotometers of crystals KBr (potassium bromide).

Scanning Electron Microscopy. Particle morphology and particle size were analysed using a scanning electron microscope (JEOL JSM 6330F - high resolution) and a high resolution (Schottky) environmental scanning electron microscope (FEI Quanta 400 FEG ESEM).

X-Ray Fluorescence. Impurities amonts were determined using a Rigaku RIX-3100 spectrometer. The samples were conformed into 25mm disks and analyzed by a semi-quantitative routine.

Raman Spectroscopy. The Raman spectroscopy used in this work was carried out in a Renishaw inVia Raman microscope. The laser applied to characterize was Helium-Neon (HeNe) laser with a wavelength λ= 633 nm and a power ~6mW. The samples were analyzed in the range of 100 cm^{-1} to 700 cm^{-1}.

Cytotoxicity Test. The positive control was phenol solution 0.5 %; the negative control was alumina 0.2 g/mL and final concentration of the extracts was 0.2g of powder per mL of culture medium. The extract was prepared with RPMI 1640 (Gibco – 23400-021) for 48h at 37°C and analyzed with DYNATECH MR4000 ELISA reader with wavelength of 490 nm. The sample was sterilized by exposure to gamma radiation (25 kGy) [16].

Results and Discussion

Table 1. XRF Semi-quantitative analysis of TiO_2 powder.

	Puritiy (%)	Cl (%)	Fe (%)	S (%)	Si (%)	Ca (%)	P (%)
500	99,7082	0,2271	0,0175	0,0163	0,0155	0,0081	0,0073

The sample of TiO_2 used in XRF showed few impurities and low levels of each one of them, also this analysis did not detect the presence of any heavy metal. With this result it is not possible to say that the material has exactly 99,71% pure, but the correct purity should be close to this value, considering the detected contaminations.

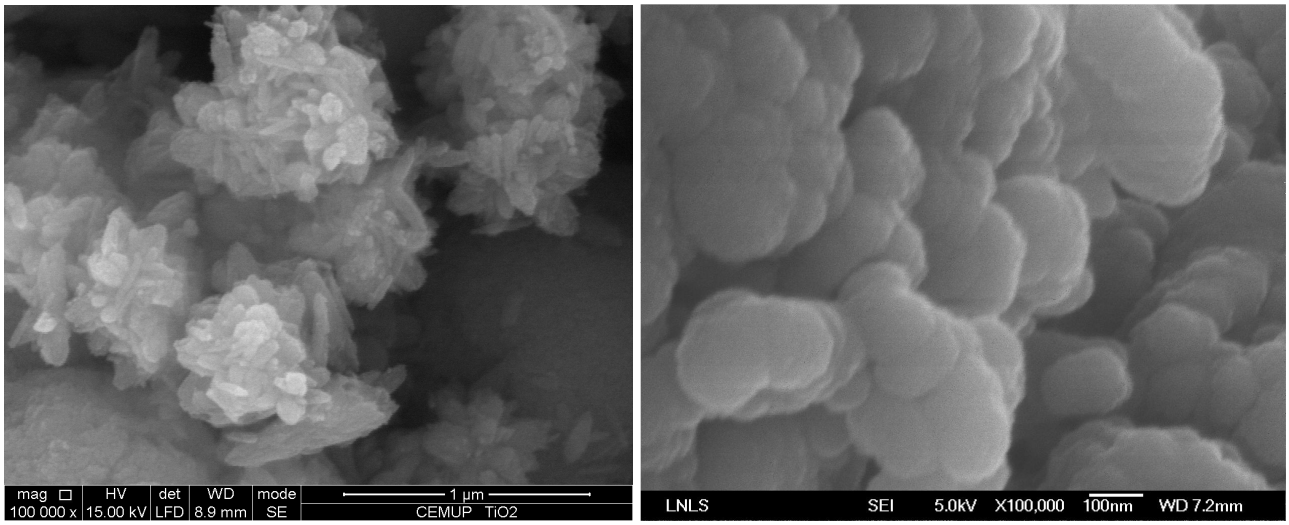

(a) (b)

Fig. 1. (a) TiO_2 without calcination. (b) TiO_2 calcinated at 500°C per 1h.

Figure 1 (a) shows the sample before calcinations and in this picture it is possible to visualize the nanoparticle size and morphology with a magnification of 100000x. Figure 1 (b) shows the agglomerated nanoparticles, but with particles size larger than the particles shown in Figure 1 (a). This is due to the temperature of the sintering heat-treatment.

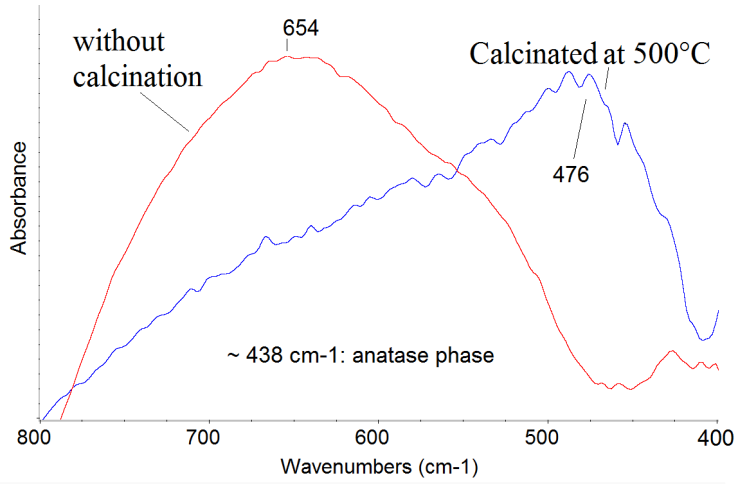

Fig. 2. FTIR TiO_2. Sample calcinated at 500°C showed the curve in 476cm^{-1} and sample without calcination showed the curve in 654cm^{-1}.

The sample calcinated at 500°C showed the dominant peak at 476 cm^{-1} corresponding to dominant anatase TiO_2 curve centered around 438 cm^{-1} [17,18] and sample without calcination showed the peak at 654 cm^{-1}. The fundamental vibrations of TiO_2 appear in the infrared spectra, which are ascribed to the stretching vibrations of Ti –O– Ti bonds in 435 – 535 cm^{-1} [19].

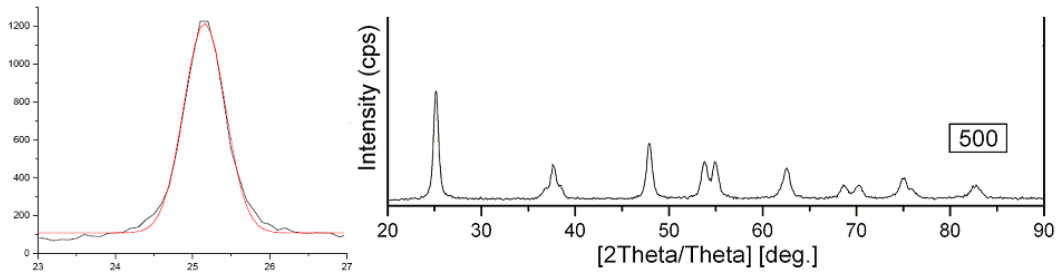

(a) (b)

Fig. 3. (a) Gaussian curve of main peak with this data: xc: 25.1559, w: 0.5371 and R^2: 0.9939. (b) XRD results of anatase TiO_2 peaks.

In Scherrer equation the gaussian curve of the main peak was used to calculate and obtain the crystallite size of the sample calcinated at for 1h. In Fig.3 (a) it is possible to visualize the data used in *Scherrer* equation (xc, w, and R^2), where, *xc* number replaces θ in equation and *w* replaces λ. The R^2 is only indicative of the accuracy of the calculus. In Fig.3 (b) the XRD results showed the correct peaks of anatase TiO_2. The main peak of this diffractogram was used to obtain the results of Fig.3 (a).

Table 2. Crystallite size of TiO_2 obtained by *Scherrer* equation:

Sample	Crystallite (nm)
TiO_2	~30

The *Scherrer* equation showed the theoretical crystalline size of TiO_2 to be approximately 30nm (Table 2).

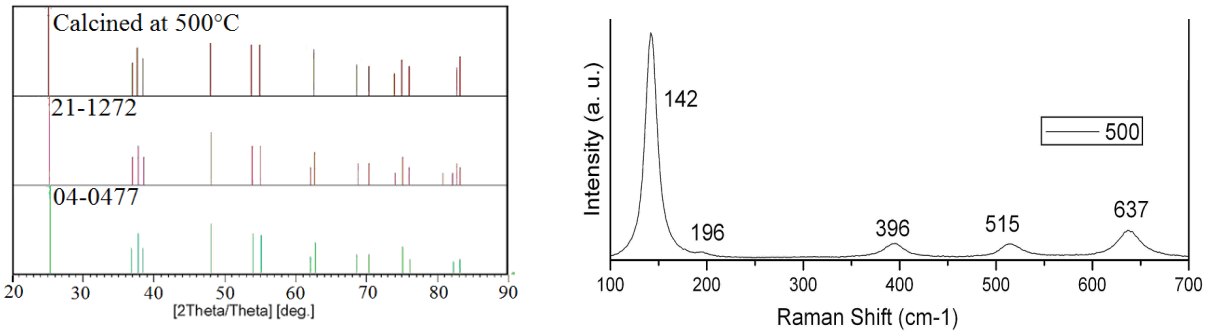

(a) (b)

Fig. 4. (a) Sample compared with standard JCPDS 21-1272 and 04-0477. (b) Bands of Anatase in Raman Spectroscopy.

Raman spectrum of nanocrystalline TiO_2 anatase phase obtained from the literature [20] is similar to the bands obtained in this work. The band 1 is at 142cm^{-1}, band 2 is at 196 cm-1, band 3 is at 396 cm^{-1}, band 4 is at 515 cm^{-1} and band 5 is at 637 cm^{-1}. This result confirms the result of XRD peaks that identifies as TiO_2 anatase.

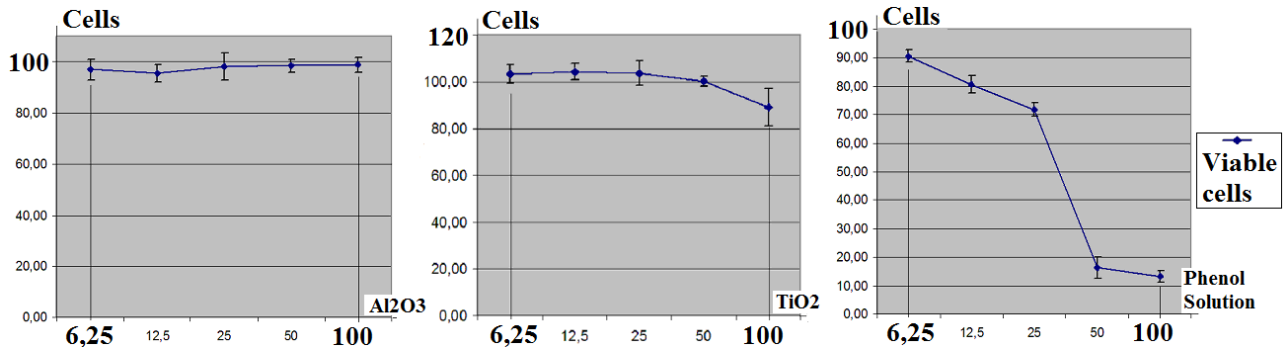

(a) (b) (c)

Fig. 5. Cytotoxicity evaluate of TiO_2 anatase powder. (a) Negative control. (b) TiO_2 sample. (c) Positive control.

The positive control was a phenol solution of 0.5 %, negative control was alumina 0.2g/mL and final concentration of the extracts was 0.2 g powder per mL of culture medium. The extract was prepared with RPMI 1640 (Gibco – 23400-021) for 48h at 37°C and analyzed with DYNATECH MR4000 ELISA reader with wavelength of 490 nm. The sample was sterilized by exposure to gamma radiation (25 kGy).

TiO_2 showed similar results with negative control which is considered a bioceramic, so we can say that anatase phase TiO_2 has the potential to be a biomaterial.

Conclusion

The XRF analysis showed interesting results since the material presented 99.7% of purity and among the few chemical elements that are contaminating the material none were heavy metals.

SEM showed the evolution of particle size and in both cases (gel and powder) nanoparticles were present. The original structure may be seen in the sample treated at 500°C based on the shape of the agglomerates present in the sample without calcination.

FTIR showed that this material is TiO_2 and confirmed, together with XRD analysis and Raman spectroscopy, that it is anatase, as resulted from comparing with two standards of JCPDS library.

The Scherrer equation used data collected from XRD diffractogram and obtained an average crystallite size of 30 nm.

With XRF and cytotoxicity test results it is possible to conclude that the synthesized titania has potential as a biomaterial.

Acknowledgments

The authors would like to thank the Brazilian Synchrotron Light Laboratory (LNLS) for SEM-FEG facilities and the Coordenação de Desenvolvimento de Pessoal de Nível Superior (CAPES) for the financial support and Dr. Vitor Baranauskas and Dr. Olga Zazuco Higa for allowing us to use their laboratory equipments.

References

[1] A. Pavlova, J. Barloti, V. Teters, J. Locs, L. Berzina-Cimdina, Processing and Application of Ceramics. 2009; 3, 4: 187–190.

[2] A. Naldoni, A. Minguzzi, A. Vertova, V. Dal Santo, L. Borgesec, C.L. Bianchi, J. Mater. Chem. 2010; 21: 400-407.

[3] Y. Li, Y. Jiang, F. Liu, F. Ren, G. Zhao, X. Leng, Food Hydrocolloids. 2011; 25, 5: 1098-1104.

[4] B.B. Topuz, G. Gündüz, B. Mavis, U. Çolak, Dyes and Pigments. 2011; 90, 2: 123-128.

[5] N. Nag, D. Guin, P. Basak, SV. Manorama, Materials Research Bulletin. 2008; 43, 12: 3270-3285.

[6] W. Yu, J. Qiu, F. Zhang, Colloids and Surfaces B: Biointerfaces. 2011; 84, 2: 400-405.

[7] J. Wang, S. Li, W. Yan, S.D. Tse, Q. Yao, Proceeding of the Combustion Institute. 2011; 33, 2: 1925-1932.

[8] P.X. Ma, Advanced Drug Delivery Reviews. 2008; 60: 184-198.

[9] X. Liu, L.A. Smith, J. Hu, P.X. Ma, Biomaterials. 2009; 30: 2252-2258.

[10] D. Qui, L. Yang, Y. Yin, A. Wang, Surface and Coatings Technology. 2011; 205, 10: 3280-3284.

[11] R. Amin, S. Hwang, S.H. Park, NANO: Brief Reports and Reviews. 2011; 6, 2: 101-111.

[12] A.E. Allounia, M.R. Cimpan, P.J. Hol, T. Skodvind, N.R. Gjerdet, Colloids and Surfaces B: Biointerfaces. 2009; 68: 83-87.

[13] K.K. Akurati, Synthesis of TiO2 based nanoparticles for photocatalytic applications. 1st edition. Cuvillier Verlag Göttingen, 2008.

[14] M. Nag, D. Guin, S.V. Manorama, Materials Research Bulletin. 2007; 9: 1691-1704.

[15] L.S. Birks, H, Friedman, Journal of Applied Physics. 1946; 17: 687-692.

[16] A.C.D. Rodas, M.J.S. Maizato, A.A. Leiner, R.N.M. Pitombo, B. Polakiewicz, M.M. Beppu, O.Z. Higa, Artificial Organs. 2008; 32, 4: 272-276.

[17] J.Y. Zhang, I.W. Boyd, B.J. O'sullivan, P.K. Hurley, P.V. Kelly, J.P. Sénateur, Journal of Non-Crystalline Solids. 2002; 303: 134-138.

[18] N. Arconada, A. Durán, S. Suárez, R. Portela, J.M. Coronado, B. Sánchez, Y. Castro, Applied Catalysis B: Environmental. 2009; 86, 1-2: 1-7.

[19] J. Wang, R.H. Li, Z.H. Zhang, W. Sun, X.F. Wang, Z.Q. Xing, R. Xu, X.D. Zhang, Inorganic Materials. 2008; 44, 6: 608-614.

[20] A. Orendorz, A. Brodyanski, J. Lösch, L.H. Bai, Z.H. Chen, Y.K. Le, C. Ziegler, H. Gnaser, Surface Science. 2007; 601: 4390-4394.